Carbohydrate Polymers 88 (2012) 562–567

Contents lists available at SciVerse ScienceDirect

Carbohydrate Polymers

journal homepage: www.elsevier.com/locate/carbpol

Surface physical and chemical properties of atmospheric pressure plasma-treated polyamideimide fibrous mats using attenuated total reflection Fourier transform infrared imaging

Gun-Young Heo, Soo-Jin Park*

Department of Chemistry, Inha University, 253 Nam-gu, Incheon 402-751, South Korea

ARTICLE INFO

Article history:
Received 22 November 2011
Received in revised form
19 December 2011
Accepted 24 December 2011
Available online 2 January 2012

Keywords:
PAI fibrous mats
Electrospinning
Atmospheric pressure plasma
ATR FT-IR
Etching effects and oxidative reactions

ABSTRACT

Fibrous mats were fabricated from polyamideimide (PAI) by electrospinning. The PAI fibrous mats were treated by atmospheric pressure plasma and the effects of the treatment power on the surface physical and chemical properties of the PAI fibrous mats were examined by attenuated total reflection Fourier transform infrared, X-ray photoelectron spectroscopy and scanning electron microscopy. The results indicated an optimum treatment condition for the surface modification of PAI fibrous mats by atmospheric pressure plasma. The concentration of chemical groups including oxygen and the surface roughness on the PAI fibrous mats increased with increasing atmospheric pressure plasma power, except at 300 W. The surface of the PAI fibrous mats became uneven after the atmospheric pressure plasma treatment, but the unevenness decreased at high plasma power. The chemical and morphological changes to the PAI fibrous mat surface before and after the atmospheric pressure plasma treatments were caused mainly by the etching effects and oxidative reactions induced by plasma processing.

1. Introduction

Nano-fiber technology is one of the most important research topics (Chinthaginjala, Thakur, Seshan, & Lefferts, 2008; Liao, Wang, Chen, & Lai, 2011; Seo & Park, 2009). Fibrous mats are porous permeable materials composed of individual non-woven polymer nano-fibers orientated randomly on a mat plane (Ma et al., 2011; Pant et al., 2011). Fibrous mats are used widely on account of their high surface area, small fiber diameter, potential to incorporate active chemistry, filtration properties, layer thinness, high permeability, and low basis weight (Ramaswamy, Clarke, & Gorga, 2011; Tan, Huang, & Wu, 2007; Nataraj et al., 2008). In recent years, the development of fibrous mats has attracted considerable research attention.

Of the many techniques for fabricating polymeric fibrous mats, electrospinning is a simple and inexpensive method for producing continuous polymeric fibers with diameters ranging from 3 nm to $\geq$5 μm compared to conventional fiber spinning (Bhardwaj & Kundu, 2010; Ramakrishna, Fujihara, Teo, Lim, & Ma, 2005). Electrospinning has two major advantages for the production of advanced polymer fibers that can lead to broad applications in traditional markets. A large quantity of nanofibers can be produced without expensive fabrication and the fiber diameter, surface-to-volume ratio, aspect ratio and pore size as non-woven fabrics can be controlled. In addition, electrospinning is applicable to a wide range of polymers, such as those used in conventional spinning, i.e. polyolefine, polyamides, polyester, aramide and acrylic. Recently, electrospinning was applied to high temperature-resistant organic polymers, such as polyamide (PA) and polyimide (PI) (Arshad, Naraghi, & Chasiotis, 2011; Schueren, Mollet, Ceylan, & Clerck, 2010; Cho, Cho, Ko, Kwon, &, Kang, 2007).

Polyamideimide (PAI) as a thermoplastic resin, is a major class of high performance engineering plastics that are used widely in electronic materials, adhesives, composite materials, fibers, and film materials as well as other engineering materials due to the excellent characteristics of the polyamides and polyimides present in its backbone, e.g. dimensional stability, thermal and mechanical properties (Margolis, 2006; Sarkar, More, Wadgaonkar, Shin, & Jung, 2007). In particular, PAI is easier to process and has better heat resistant properties than polyimide and polyamide. Many studies have examined the applications of PAI, such as filtration media, electrical insulating wires and reinforcements (Rajesh, Maheswari, Senthilkumar, Jayalakshmi, & Mohan, 2011).

Considerable research effect has been made to improve interfacial properties and achieve fibrous mats with good properties. From this point of view, surface treatment is generally used to improve the adhesion and filtration properties at the interface between nano-fibers (Guo et al., 2009). Atmospheric pressure

* Corresponding author.
E-mail address: sjpark@inha.ac.kr (S.-J. Park).

0144-8617/$ – see front matter.
doi:10.1016/j.carbpol.2011.12.038

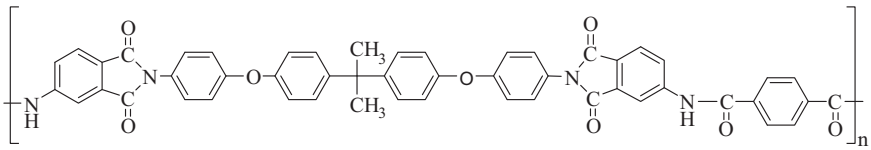

PAI

Fig. 1. Chemical structure of PAI.

plasma treatment is currently used for chemical modification of polymer materials owing to its low cost, good environmental sustainability, high efficiency and low energy consumption (Kuoa, Chang, Hung, Chen, & Inagaki, 2010; Shi et al., 2011). The effects of the atmospheric pressure plasma power on surface characteristics of fibrous mats have received less attention and there are no reports on the surface properties of atmospheric pressure plasma treated-fibrous mats using attenuated-total-reflection Fourier-transform infrared (ATR FT-IR) imaging (Cheng et al., 2010; Jiang et al., 2009).

In this study, electrospinning was used to prepare fibrous mats from a PAI solution. The effects of an atmospheric pressure plasma treatment on the surface characteristics of PAI fibrous mats were investigated by ATR FT-IR spectroscopy and scanning electron microscopy (SEM). The surface chemical composition and surface functionality of the PAI fibrous mats were analyzed by X-ray photoelectron spectroscopy (XPS).

2. Experimental

2.1. Materials

PAI was synthesized according to the method reported by Hong, Suh, Kim, and Choi (1998), using diimide diamines (DIDA) and terephthalic acid (TPA) as a diacid by direct polycondensation from an equimolar amount of thionyl chloride (TC) in N-methyl-2-pyrrolidone (NMP) at room temperature. All organic starting materials used for synthesis were purchased from Aldrich Chemical Co. and Merck Co. and all reagents were used as received. Fig. 1 shows the chemical structure of PAI. PAI was dissolved in dimethyl formamide (DMF) and stirred for 3 h at approximately 60 °C. The PAI concentration in DMF was approximately 25 wt.%.

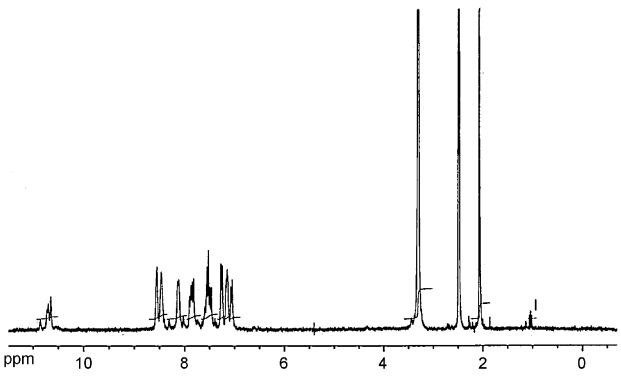

Fig. 2. ^{1}H NMR spectrum of PAI.

Table 1
Conditions used for atmospheric pressure plasma.

	Conditions
Gas	Helium (15 L/min)/air (0.5 L/min)
Nozzle distance	3 mm
Plasma power	100 W, 200 W, 300 W

2.2. Synthesis of PAI

A two-step method was used to synthesize PAI preparation of the monomer intermediate and polymerization, followed by a typical procedure. 2,2-Bis[4-(4-aminophthalimidophenoxy) phenyl]propane (BAPP) as the monomer for the synthesis of PAI was prepared using the method reported by Hong et al. (1998) as follows.

Thionyl chloride (13.08 g, 0.11 mol) was added to NMP (200 mL) in an ice-water bath and stirred for 10 min. TPA (8.31 g, 0.05 mmol) in NMP (200 mL) was then added at once, and the resulting mixture was stirred at room temperature for 40 min. Subsequently, 35.09 g (0.05 mmol) of BAPP in 200 mL of NMP was added. An exothermic reaction occurred but the reaction temperature was maintained at room temperature for 4 h. The by-product, HCl, was removed by adding propylene oxide (11.02 g, 0.22 mmol) and the reaction was allowed to proceed at room temperature for 2 h. The resulting viscous mixture was poured rapidly, into methanol with constant stirring in a Waring Blender. The final products were washed with water and methanol, collected by filtration and dried at 120 °C under reduced pressure for 24 h.

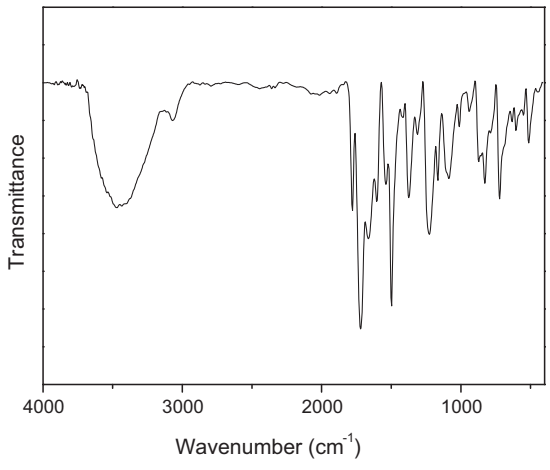

Fig. 3. FT-IR spectrum of PAI.

Table 2
Chemical characterization.

Analysis method	Chemical characterization
FT-IR (KBr, cm^{-1})	1721 ($\upsilon_{C=O}$), 1663 ($\upsilon_{C=O}$), 1601 (υ_{C-N}), 1374 (υ_{C-N}), 3431 (υ_{N-H})
^{1}H NMR (DMSO-d_6)	2.49 (s, H), 7.00 (s, H), 7.15 (s, H), 7.27 (s, H), 7.46 (s, H), 7.75 (s, H), 7.96 (s, H), 8.16–8.22 (d, 2H), 8.45 (s, H), 8.61 (s, H), 10.65 (s, NH)

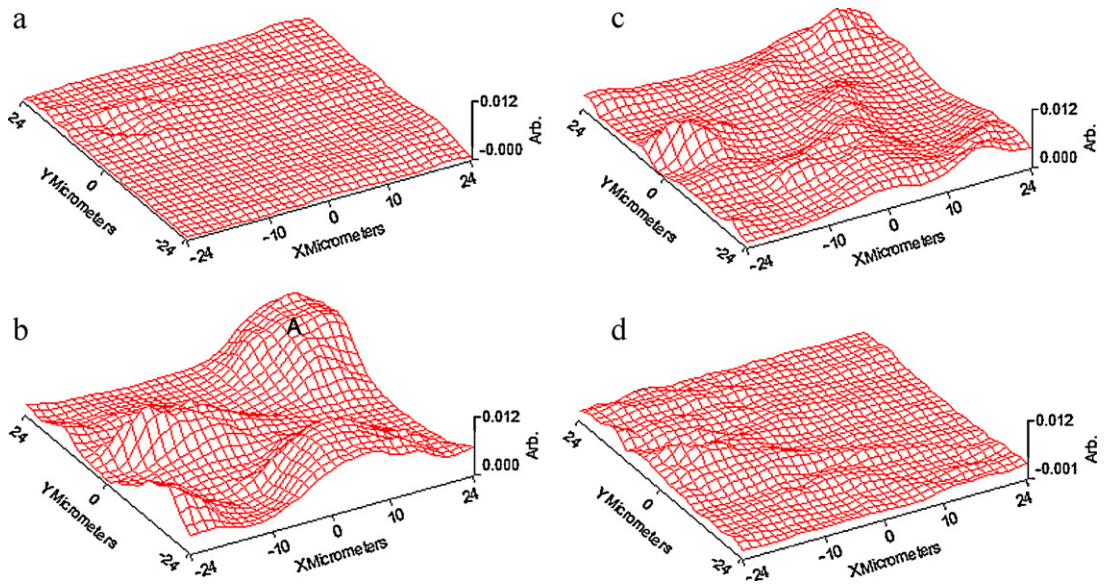

Fig. 4. ATR FT-IR spectroscopic images. (a) Raw PAI fibrous mats; (b) PAI fibrous mat treated by 100 W; (c) PAI fibrous mat treated by 200 W; (d) PAI fibrous mat treated by 300 W.

2.3. Electrospinning process

Electrospinning was carried out at room temperature using a 10 mm inner diameter glass syringe with a 15 cm working distance. The resulting polymer solution was spun into a fiber web using an electrospinning apparatus equipped with a power supply (SHV-200 Series 200 W, Conver Tech Co.). The solution was ejected from a syringe tip onto aluminum foil that had been wrapped on a metal drum rotating at approximately 300 rpm. Electrospinning was carried out at 19 kV and the fibers were dried at room temperature for 24 h.

2.4. Atmospheric pressure plasma treatment

An atmospheric pressure plasma treatment of the electrospun PAI fibrous mats was carried out at different plasma powers. The PAI fibrous mats were placed in the center of the chamber at atmospheric pressure. Helium was used as a carrier gas and air was used as the reactive gas. Both gases were of 99.99% purity. The treatment was carried out in a helium (15 L/min)/air (0.5 L/min) atmospheric pressure plasma discharge for up to 1 min. The sample to nozzle distance was 3 mm. The samples were treated with the atmospheric pressure plasma at between 100 and 300 W. The conditions used for atmospheric pressure plasma treatment are listed in Table 1.

2.5. ATR FT-IR spectroscopic imaging

ATR FT-IR (PerkinElmer Spectrum Spotlight 400) analyses were performed to examine the effect of the atmospheric pressure plasma power on the surface properties of the PAI fibrous mats. The spectra were recorded over the 4000–680 cm^{-1} range with a resolution of 2 cm^{-1} and 32 scans. The imaging area was 50 μm × 50 μm.

Table 3
Atomic composition of PAI fibrous mat surfaces before and after atmospheric pressure plasma treatment.

Sample	Atomic conc.%		
	C_{1s}	O_{1s}	O_{1s}/C_{1s}
Raw PAI fibrous mats	84.73	15.27	0.1802
PAI fibrous mat treated by 100 W	79.30	20.70	0.2610
PAI fibrous mat treated by 200 W	83.14	16.86	0.2028
PAI fibrous mat treated by 300 W	83.65	16.35	0.1955

2.6. XPS

The elemental composition of the electrospun PAI fibrous mats after the different surface treatments was examined by XPS (Thermo Scientific K-Alpha) using monochromated Al Kα X-rays (1486.6 eV). The analyzer pass energy was 200 eV for the high-resolution core-level spectra and the beam spot was 400 μm.

2.7. SEM

The morphology and structure of the electrospun PAI fibrous mats were observed by SEM (Hitachi S-4200).

3. Results and discussion

3.1. Characterization of synthesized PAI as a precursor for fibrous mats

PAI was prepared from an equimolar amount of BAPP and terephthalic acid via a direct polycondensation reaction using

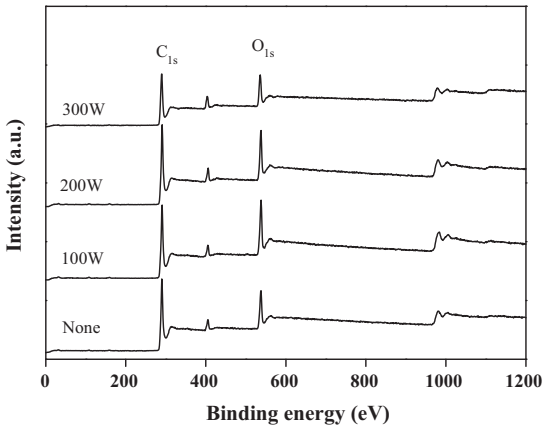

Fig. 5. XPS spectra of the PAI fibrous mats.

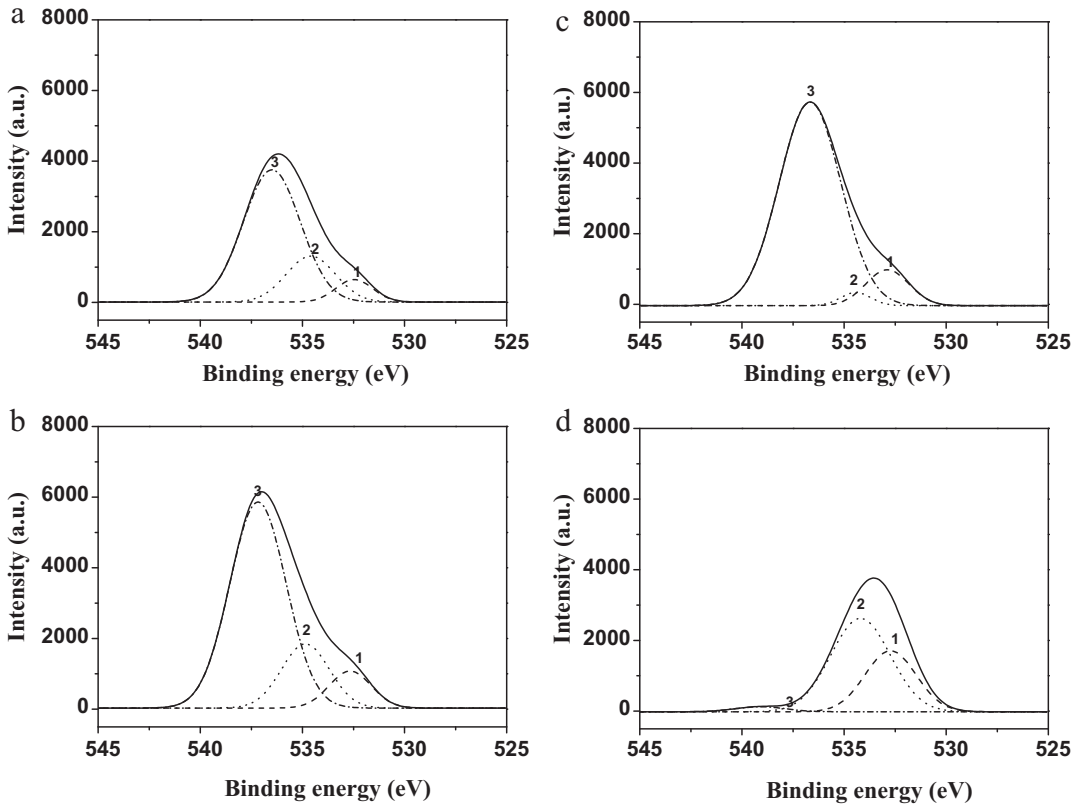

Fig. 6. High-resolution spectra of the O_{1s} peaks. (a) Raw PAI fibrous mats; (b) PAI fibrous mat treated at 100 W; (c) PAI fibrous mat treated at 200 W; (d) PAI fibrous mat treated at 300 W.

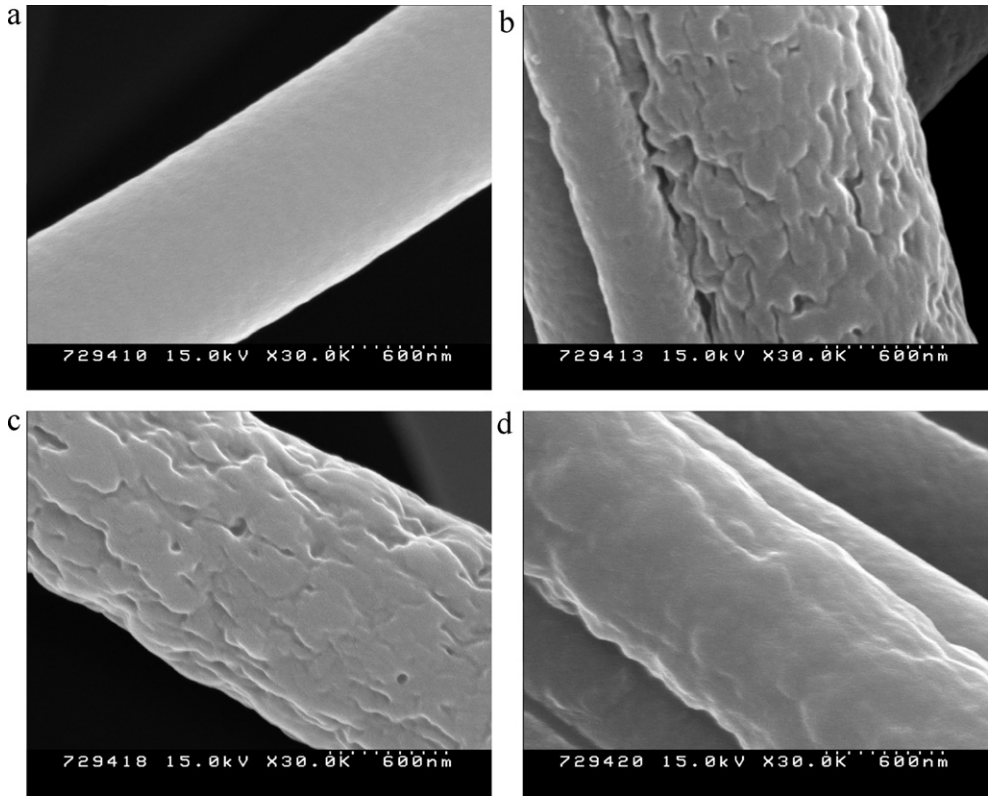

Fig. 7. SEM images of the PAI fibrous mats. (a) Raw PAI fibrous mats; (b) PAI fibrous mat treated at 100 W; (c) PAI fibrous mat treated at 200 W; (d) PAI fibrous mat treated at 300 W.

thionyl chloride (TC) in NMP at room temperature. The structure of the monomer was confirmed by ^{1}H nuclear magnetic resonance (^{1}H NMR), FT-IR spectroscopy and elemental analysis. Figs. 2 and 3 show ^{1}H NMR and FT-IR spectra of the synthesized PAI, respectively, and the results are summarized in Table 2.

As shown in Fig. 2 and Table 2, the ^{1}H NMR spectra of the PAI exhibited a multiplet between 6.55 and 8.75 ppm corresponding to the aromatic protons of BAPP and TPA, and the proton signal of amide N—H appeared in the range, 10.65 ppm. FT-IR revealed absorption bands at 3431 (amide, N—H), 1780 (imide, symmetric C=O stretching), 1721 (acid C=O stretching and asymmetric imide C=O stretching), 1374 (C—N stretching vibration), 1186 (imide ring deformations), and 732 cm^{-1} (imide ring deformations), confirming the presence of an imide ring and carboxylic acid group in the structure.

3.2. ATR FT-IR spectroscopic imaging

ATR FT-IR spectroscopy was used to determine the effects of the atmospheric pressure plasma treatment of the PAI fibrous mats. This method can be used to determine the change in functional groups of a substance (Josepha et al., 2010). Many functional groups changed in this atmospheric pressure plasma system, and each has different absorption bands that can be used for identification. The bands of hydroxyl group were used to confirm the effect of the atmospheric pressure plasma treatment on surface characteristics of the PAI fibrous mats.

The band corresponding to the stretching modes of hydroxyl and ether groups (3600–3200, 1100–1000 cm^{-1}) was used to monitor the surface characteristics of the PAI fibrous mats at 100–300 W. Fig. 4 shows the images converted using these bands at different atmospheric pressure plasma powers. The uniform distribution of hydroxyl and ether groups can be distinguished easily using this method from the spectral intensity differences. The atmospheric pressure plasma-treated PAI fibrous mats showed a significantly higher absorption intensity of hydroxyl and ether groups than the raw PAI fibrous mats, except 300 W.

The absorption intensity of the PAI fibrous mat treated at 100 W was higher than that of the other PAI fibrous mats. On the other hand, the PAI fibrous mats treated at 100 W showed a hydroxyl and ether group-rich region (areas A of image (b) in Fig. 4) that was distributed non-uniformly. In contrast, the absorption intensity of the PAI fibrous mats treated at 200 W (image (c) in Fig. 4) showed a low absorption intensity of hydroxyl groups but a more uniform distribution. The spatial distribution of hydroxyl groups did not show any noticeable change when the PAI fibrous (image (d) in Fig. 4) was exposed to 300 W. Therefore, the intensity of hydroxyl and ether groups showed a maximum at 100 W, and the distribution of hydroxyl and ether groups in the PAI fibrous mats became more uniform with increasing atmospheric pressure plasma power.

3.3. XPS

XPS was used to confirm the ATR FT-IR measurements by examining closely the surface characteristics of the atmospheric pressure plasma-treated PAI fibrous mats. Fig. 5 presents the XPS spectra of the PAI fibrous mat surfaces before and after the atmospheric pressure plasma treatment. The atomic composition of the untreated and the atmospheric pressure plasma-treated PAI fibrous mats was determined from Fig. 5, and the results are listed in Table 3.

As shown in Table 3, the untreated PAI fibrous mats contained 15.27% oxygen and 84.73% carbon, whereas the atmospheric pressure plasma-treated PAI fibrous mats contained 16.35–20.70% oxygen and 83.65–79.30% carbon. This suggests that the O_{1s}/C_{1s} ratios of the atmospheric pressure plasma-treated PAI fibrous mats were higher than those of untreated PAI fibrous mats. This result is due to the facts that the air gas as a reactive gas promotes surface oxidation and hydroxylation on PAI fibrous mats. On the other hand, the O_{1s}/C_{1s} ratio of the atmospheric pressure plasma-treated PAI fibrous mats showed a maximum ratio at 100 W, which decreased with further increases in atmospheric pressure plasma power.

The high-resolution XPS spectra of the O_{1s} peaks were examined closely to identify the chemical groups introduced to the surface of the PAI fibrous mats by the atmospheric pressure plasma treatment. The core level spectra were fitted to mixed Gaussian–Lorentzian components (Fig. 6). The O_{1s} XPS peak of the PAI fibrous mat surfaces before and after the atmospheric pressure plasma treatment was observed at 528–542 eV, and was composed of three main components. Peak 1, at a binding energy of ~532 eV, was assigned to carbonyl oxygen (C=O or —COOH) of the PAI fibrous mats and "free" carbonyl groups generated by the plasma treatments. Peak 2, at a binding energy of ~535 eV, corresponded to the bridging oxygen atoms (C—O—C) of the PAI fibrous mats. Peak 3 of O_{1s}, at a binding energy of ~536 eV, was attributed to ether groups (C—O—C) and hydroxyl groups (—OH) generated by the plasma treatments.

As shown in Fig. 6, the intensity of peaks 1 and 3 increased when exposed to the atmospheric pressure plasma up to 200 W, but the intensity of peak 3 decreased significantly above 300 W. This is because high plasma power can interrupt the linkage of the ester chain and the formation of hydroxyl groups on the surface of the PAI fibrous mats (Josepha et al., 2010). Therefore, at 300 W, the peak for carbonyl oxygen (C=O or —COOH) increased but that of the ether groups (C—O—C) and hydroxyl groups (—OH) generated by the plasma treatments decreased.

3.4. SEM

SEM was used to determine the effect of the atmospheric pressure plasma power on the surface morphology of the of PAI fibrous mats. Fig. 7 presents SEM images before and after the atmospheric pressure plasma treatment.

As shown in Fig. 7, the surface of the PAI fibrous mats after the atmospheric pressure plasma treatment (Fig. 7(b)–(d)) was uneven and clearly different from that of the untreated PAI fibrous mats (Fig. 7(a)), which was clean and smooth. After the fiber was treated by atmospheric pressure plasma, the surface of the PAI fibrous mats appeared uneven with apparent bulges and ruts. In contrast, at high plasma power (Fig. 7(d)), the surface became less uneven due to etching effects and oxidative reactions (Yoon, Moon, Lyoo, Lee, & Park, 2009). This shows that high power plasma treatment induces etching effects and oxidative reactions on the surface of the PAI fibrous mats.

4. Conclusion

A high power atmospheric pressure plasma treatment (300 W) produced a uniform distribution of chemical groups on PAI fibrous mats but the content of chemical groups including oxygen was lower than that produced at lower powers. The surface roughness of PAI fibrous mats increased with increasing the atmospheric pressure plasma power, except at 300 W. The changes to the PAI fibrous mat surface before and after the atmospheric pressure plasma treatments were caused mainly by etching effects and oxidative reactions induced by plasma processing.

Acknowledgment

This study was supported by the Carbon Valley Construction Project.

References

Arshad, S. N., Naraghi, M., & Chasiotis, I. (2011). Strong carbon nanofibers from electrospun polyacrylonitrile. *Carbon*, *49*, 1710–1719.

Bhardwaj, N., & Kundu, S. C. (2010). Electrospinning: A fascinating fiber fabrication technique. *Biotechnology Advances*, *28*, 325–347.

Cheng, S. Y., Yuen, C. W. M., Kan, C. W., Cheuk, K. K. L., Daoud, W. A., Lam, P. L., et al. (2010). Influence of atmospheric pressure plasma treatment on various fibrous materials: Performance properties and surface adhesion analysis. *Vacuum*, *84*, 1466–1470.

Chinthaginjala, J. K., Thakur, D. B., Seshan, K., & Lefferts, L. (2008). How carbon-nanofibers attach to Ni foam. *Carbon*, *46*, 1638.

Cho, C. W., Cho, D. H., Ko, Y. G., Kwon, O. H., & Kang, I. K. (2007). Stabilization, carbonization, and characterization of PAN precursor webs processed by electrospinning technique. *Carbon Letters*, *8*, 313–320.

Guo, H., Huang, Y. D., Meng, L. H., Liu, L., Fan, D. P., & Liu, D. X. (2009). Interface property of carbon fibers/epoxy resin composite improved by hydrogen peroxide in supercritical water. *Materials Letters*, *63*, 1531–1534.

Hong, Y. T., Suh, D. H., Kim, S. Y., & Choi, K. Y. (1998). Synthesis and characterization of new poly(amide imide)s by direct polycondensation of diamine containing diimide group and diacids using thionyl chloride. *Angewandte Makromolekulare Chemie*, *259*, 39–44.

Jiang, Q., Li, R., Sun, J., Wang, C., Peng, S., Ji, F., et al. (2009). Influence of ethanol pretreatment on effectiveness of atmospheric pressure plasma treatment of polyethylene fibers. *Surface & Coatings Technology*, *203*, 1604–1608.

Josepha, E., Ricci, C., Kazarianb, S. G., Mazzeoa, R., Prati, S., & Ioele, M. (2010). Macro-ATR-FT-IR spectroscopic imaging analysis of paint cross-sections. *Vibrational Spectroscopy*, *53*, 274–278.

Kuoa, Y. L., Chang, K. H., Hung, T. S., Chen, K. S., & Inagaki, N. (2010). Atmospheric-pressure plasma treatment on polystyrene for the photo-induced grafting polymerization of N-isopropylacrylamide. *Thin Solid Films*, *518*, 7568–7573.

Liao, C. C., Wang, C. C., Chen, C. Y., & Lai, W. J. (2011). Stretching-induced orientation of polyacrylonitrile nanofibers by an electrically rotating viscoelastic jet for improving the mechanical properties. *Polymer*, *52*, 2263–2275.

Ma, G., Liu, Y., Peng, C., Fang, D., He, B., & Nie, J. (2011). Paclitaxel loaded electrospun porous nanofibers as mat potential application for chemotherapy against prostate cancer. *Carbohydrate Polymers*, *86*, 505–512.

Margolis, J. M. (2006). *Engineering plastics handbook*. New York: McGraw-Hill., p. 257.

Nataraj, S. K., Kim, B. H., Yun, J. H., Lee, D. H., Aminabhavi, T. M., & Yang, K. S. (2008). Electrospun nanocomposite fiber mats of zinc-oxide loaded polyacrylonitrile. *Carbon Letters*, *9*, 108–114.

Pant, H. R., Neupane, M. P., Pant, B., Panthi, G., Oh, H. J., Lee, M. H., et al. (2011). Fabrication of highly porous poly (ε-caprolactone) fibers for novel tissue scaffold via water-bath electrospinning. *Colloids and Surfaces B: Biointerfaces*, *88*, 587–592.

Rajesh, S., Maheswari, P., Senthilkumar, S., Jayalakshmi, A., & Mohan, D. (2011). Preparation and characterisation of poly(amide-imide) incorporated cellulose acetate membrane for polymer enhanced ultrafiltration of metal ions. *Chemical Engineering Journal*, *171*, 33–44.

Ramakrishna, S., Fujihara, K., Teo, W., Lim, T., & Ma, Z. (2005). *An introduction to electrospinning and nanofibers*. Singapore: World Scientific Publishing.

Ramaswamy, S., Clarke, L. I., & Gorga, R. E. (2011). Morphological, mechanical, and electrical properties as a function of thermal bonding in electrospun nanocomposites. *Polymer*, *52*, 3183–3189.

Sarkar, A., More, A. S., Wadgaonkar, P. P., Shin, G. J., & Jung, J. C. (2007). Synthesis and liquid-crystal-aligning properties of novel aromatic poly(amide imide)s bearing n-alkyloxy side chains. *Journal of Applied Polymer Science*, *105*, 1793–1801.

Schueren, L. V., Mollet, T., Ceylan, O., & Clerck, K. D. (2010). The development of polyamide 6.6 nanofibres with a pH-sensitive function by electrospinning. *European Polymer Journal*, *46*, 2229–2239.

Seo, M. K., & Park, S. J. (2009). Electrochemical characteristics of activated carbon nanofiber electrodes for supercapacitors. *Materials Science and Engineering B*, *164*, 106–111.

Shi, Q., Vitchuli, N., Nowak, J., Lin, Z., Guo, B., Mccord, M., et al. (2011). Atmospheric plasma treatment of pre-electrospinning polymer solution: A feasible method to improve electrospinnability. *Journal of Polymer Science. Part B: Polymer Physics*, *49*, 115–122.

Tan, S., Huang, X., & Wu, B. (2007). Some fascinating phenomena in electrospinning processes and applications of electrospun nanofibers. *Polymer International*, *56*, 1330–1339.

Yoon, Y. I., Moon, H. S., Lyoo, W. S., Lee, T. S., & Park, W. H. (2009). Superhydrophobicity of cellulose triacetate fibrous mats produced by electrospinning and plasma treatment. *Carbohydrate Polymers*, *75*, 246–250.